Materiales de Construcción
Vol. 70, Issue 340, October–December 2020, e234
ISSN-L: 0465-2746
https://doi.org/10.3989/mc.2020.12719

A study on industrial-scale waste utilization in construction material production: the use of fly ash in GRP composite pipe

A. Beycioğlu[a]✉, H. Mis[b], E.D. Güner[c], H. Güner[b], N. Gökçe[b]

a. Department of Civil Engineering, Adana Alparslan Türkeş Science and Technology University, (Adana, Turkey)
b. Superlit Pipe Industry Inc. Düzce Factory R&D Department, (Düzce, Turkey)
c. Department of Environmental Engineering, Çukurova University, (Adana, Turkey)
✉ abeycioglu@atu.edu.tr

Received 12 September 2019
Accepted 24 July 2020
Available on line 15 October 2020

ABSTRACT: This study presents a new approach to the utilization of industrial by-products in construction materials by using fly ash (FA) in the production of glass fiber-reinforced polyester (GRP) pipe. The FA was substituted by 10% and 20% (by weight of sand) in the mixtures to produce GRP pipes of 350 mm in diameter and 6 m in length for testing. Stiffness modulus (SM), axial tensile strength (ATS), and hoop tensile strength (HTS) tests were conducted on the produced GRP pipes and their elasticity modulus (EM) values were also calculated. To observe the microstructure of the GRP pipes and the interfacial transition zone of the layers, SEM and microscopic analyses were performed. Furthermore, a strain-corrosion test was conducted to obtain information about long term-performance of samples. The results showed that the FA-filled GRP pipes were found to meet the requirements of the related standards, and that the use of FA in the GRP pipe industry may be an important alternative approach to the utilization of industrial wastes via effective recycling mechanisms.

KEYWORDS: Composite; Fly ash; Polymer; Durability; Mechanical properties.

Citation/Citar como: Beycioğlu, A.; Mis, H.; Güner, E.D.; Güner, H.; Gökçe, N. (2020) A study on industrial-scale waste utilization in construction material production: the use of fly ash in GRP composite pipe. Mater. Construcc. 70 [340], e234 https://doi.org/10.3989/mc.2020.12719

RESUMEN: *Estudio sobre la utilización de residuos a escala industrial en la producción de materiales de construcción: empleo de cenizas volantes en tuberías compuestas de GRP.* Este estudio experimental presenta un nuevo enfoque para la utilización de subproductos industriales en materiales de construcción mediante el uso de cenizas volantes (FA) en la producción de tubos de poliéster reforzado con fibra de vidrio (GRP). Para las pruebas, se sustituyeron 10% y 20% de FA (en peso de arena) en las mezclas para producir tuberías de GRP de 350 mm de diámetro y 6 m de longitud. Se realizaron pruebas de módulo de rigidez (SM), resistencia a la tracción axial (ATS) y resistencia a la tensión del aro (HTS) en las tuberías de GRP producidas y también se calcularon sus valores de módulo de elasticidad (EM). Para observar la microestructura de las tuberías de GRP y la zona de transición interfacial de las capas, se realizaron análisis de microscópia y SEM. Además, se realizó una prueba de corrosión por deformación para obtener información sobre el rendimiento a largo plazo de las muestras. Los resultados mostraron que las tuberías de GRP rellenas de FA cumplían con los requisitos de los estándares relacionados, y que el uso de FA en la industria de tuberías de GRP puede ser un enfoque alternativo importante para la utilización de desechos industriales a través de mecanismos de reciclaje efectivos.

PALABRAS CLAVE: Composite; Cenizas volantes; Polímero; Durabilidad; Propiedades mecánicas.

ORCID ID: A. Beycioğlu (https://orcid.org/0000-0001-6287-1686); H. Mis (https://orcid.org/0000-0001-9086-298X); E.D. Güner (https://orcid.org/0000-0002-0492-2999); H. Güner (https://orcid.org/0000-0002-9876-1718); N. Gökçe (https://orcid.org/0000-0001-5418-0551)

1. INTRODUCTION

Fly ash is a by-product constituting about 60–88% of the total combustion residues from coal-fired electric generating plants and is recognized as an environmental pollutant. Since the increase of energy production facilities due to rising energy demands in developing countries, FA is rapidly becoming a very serious environmental problem. From the environmental perspective, the recycling of FA is as important as energy production and thus, the disposal of this by-product has long attracted the attention of researchers (1, 2). Commonly used disposal methods have included depositing the FA in landfills or just dumping it as waste. Disposal of solid wastes in landfills requires more storage space and also causes additional carbon emissions, leading to serious environmental issues. Consequently, this method has recently become less attractive (1, 3, 4). Over the past few decades, various approaches have been studied to find the best solution for FA utilization.

Research carried out on the reuse of FA as an alternative to landfill disposal covers a wide number of fields, ranging from agriculture to engineering. Bicer (5) used FA as a sand replacement in concrete and plaster and investigated the impact of FA grain size on the thermal and mechanical performance of the composite material. Cheng et al. (6) used isotropically consolidated drained (CID) triaxial tests to examine the stress-dependent behavior of marine clay admixed with fly ash-blended cement (FAC). Martin et al. (7) studied the effect of FA on the hydration of calcium sulfoaluminate cement. Güllü et al. (8) experimentally investigated the rheological capability of geopolymer material for grouting in comparison with grouts including FA and geopolymer aggregate. Duan et al. (9) examined the relevance of ultrafine FA properties and mechanical properties in fly ash-cement gelation blocks via static pressure forming. Ren and Sancaktar (10) studied the use of FA as a filler in synthetic rubber for tire applications. Zhang et al. (11) investigated the flexural and ductile failure of carbonized concrete containing different proportions of FA and active magnesium oxide. Sun and Vollpracht (12) presented a study on the time-dependent behavior of sodium silicate-activated FA and metakaolin geopolymers. Wang and Lu (13) studied the resistivity of FA concrete and the rebar corrosion rate in FA-substituted concrete. Hadi et al. (14) examined the properties of FA-based geopolymer mortar. Hefni et al. (15) sought to solve the low early strength problem via chemical activation of Class F fly ash. Bahedh and Jaafar (16) studied some of the properties of ultra-high-performance concrete produced by utilizing FA via autoclaving. Gökçe et al. (17) reported on the properties of foam concrete containing FA. Uysal et al. (18) studied geopolymer paste composed of FA, ground glass fiber, and glass powder. Atis et al. (19) investigated the use of a non-standard high-calcium FA in concrete. Irassar and Batic (20) studied the sulfate resistance of ordinary Portland cement with FA. Fernández-Jiménez et al. (21) experimentally investigated the effect of the NaOH, KOH, Na_2CO_3 K_2CO_3, sodium silicate, and potassium silicate as alkaline activators in the microstructural development of thermal-alkali activated FA systems. Woszuk et al. (22) used Class F and Class C fly ash as a partial replacement for the filler in asphalt. Yan et al. (23) utilized FA from the municipal solid waste incinerator as a replacement for the traditional limestone mineral filler in bitumen mortar and found that the FA improved the high-temperature performance of the asphalt binder.

The recycling/utilization of FA has a number of environmental benefits, including reduced landfill disposal, reduced consumption of virgin resources, and reduced greenhouse gas emissions (24). Direct utilization is among the desirable methods for the recycling of hazardous industrial wastes like FA, and since direct utilization of FA is low in cost, it has become a prominent strategy for industrial companies. Fly ash utilization also reduces the need for additional landfill space and conserves natural resources (2). Experiences gained in recycling indicate that recycling wastes through incorporation of them into useful products is possible; however, the actions necessary to reach industrial-scale solutions for recycling of these wastes via effective technologies are very important. Reducing waste using mechanical, thermal, and chemical approaches is increasingly being considered by various industrial sectors (25).

Glass fiber-reinforced polyester (GRP) composite pipes are used in a number of civil engineering applications such as transporting clean and potable water, water for irrigation, for hydroelectric power plants, and for water treatment, water storage, and sewer systems, for storm water and seawater intake and discharge, and for trenchless technologies. Due to this wide area of application, the direct utilization by the GRP pipe sector of a large amount of by-products can be regarded as an industrial-scale solution (26, 27).

2. MATERIAL AND METHODS

In the experimental stage, GRP pipes were produced using silica sand as a filling material, glass fiber as a reinforcing material, cobalt octoate as an accelerator, methyl-ethyl ketone peroxide as an initiator, and orthophthalic unsaturated polyester resin (with the characteristic of thermoset) as a binder. Two types of resins were used in the production of the inner and outer layers of the GRP pipes. The liner resin, having high chemical resistance, was used

in the first 1-mm thickness of the inner surface. The orthophthalic polyester resin was used to produce the other layers of the GRP pipes. Properties of the resins used in this study are presented in Table 1.

E-glass fiber with a length of ~25–50 mm was used as a reinforcing material. In the production of the GRP pipes, silica sand was used as a filler material to increase the rigidity. Table 2 summarizes the properties of the silica sand (maximum size, 0.85 mm).

The FA, a by-product obtained from the Çatalağzı thermal power plant (in Turkey), was substituted for silica sand in the mixtures by amounts of 10% and 20% to form the structural layers of the GRP pipes. The FA used in the study contained the following oxides: SiO_2 (55.16%), Fe_2O_3 (5.70%), TiO_2 (1.11%), Al_2O_3 (26.79%), CaO (1.91%), MgO (1.15%), Na_2O (0.43%), K_2O (4.94%), SO_3 (0.001%) and P_2O_5 (0.24%). Prior to the production process, the silica sand and FA were mixed (135 kg silica sand + 15 kg FA for the 10% FA substitution and 120 kg silica sand + 30 kg FA for the 20% FA substitution) by mechanical mixing methods in a large container and placed into the bulk trailer of the centrifugal casting (CC) system. Three types of GRP composite pipes were produced in this study. One of them was the reference pipe (REF) produced without FA, while the others contained 10% and 20% FA. The GRP pipes were produced on a one-to-one scale under PN 6 bar pressure class and SN 5000 N/m^2 stiffness class. All pipes were manufactured by the CC method operating with a PLC-PC fully automatic controlled system (Figure 1a). In the production of the pipes, the materials were fed to the rotating mold via a feeder (Figure 1b). Initially, the mold was rotated relatively slowly. When the feeding of all the raw materials was completed, the cast rotation speed was increased in order to achieve adequate compression. By increasing the rotation speed of the mold, full compression and transition to a solid material (curing) were ensured. The wall thickness of the pipe was manufactured layer-by-layer by the reciprocating motion of the feeder within the mold. Glass fibers, acting as reinforcing material, were placed on both sides of the neutral axis on the pipe wall, and the gap remaining in-between was filled with silica sand + FA, resin, and glass fiber. After production using the CC method, the pipes were removed from the rotating mold. The GRP pipe samples manufactured with FA are shown in Figure 1c.

The resin was designed to be non-polymerized during the pipe production. For the pipe production, the fibers used were cut in lengths of 25–50 mm. The 10% FA-substituted GRP pipe produced in this study is given in Figure 2 with cross-sectional details. In the cross-section, the external surface protective layer (numbered as 1) and the body core of the structural layer (numbered as 5 and 6) were producing using the FA- silica sand admixture.

After producing the pipes, test samples were prepared according to the ISO 7685 standard for SM, ISO 8521 standard for HTS, and ISO 8513 standard for ATS. Details of all tests applied to the GRP pipes are given in Table 3.

After preparing the samples detailed in Table 5, HTS (Figure 3a), ATS (Figure 3b) and SM (Figure 3c) tests were performed on the produced pipes according to the related standards. Some dimensional details of test samples are also given in Figure 3d-e.

By using the ultimate forces (F) obtained from the test machine, the HTS and ATS were calculated using Equations [1] and [2], respectively.

$$HTS = \frac{F}{2.w} \quad [1]$$

$$ATS = \frac{F}{w} \quad [2]$$

Table 2. Properties of silica sand used in this study.

Parameter	Result
Resin and Sand Mix Gel Time	07.15 min
Moisture Content (@105 °C, 2 h)	0.03%
Bulk Density	1.52 g/cm^3
Particle Size & Distrubution	0.81%
Loss on Ignition	0.13%

Table 1. Properties of resins used in this study.

Parameter	Test Method	Orthophthalic Polyester Resin (Body)	Polyester Resin (Liner)
Viscosity (@25 °C)	ASTM D 2196	225 cp	570 cp
GelTime (@25 °C)	ASTM D 3056	11 min	12 min.
Exotherm Peak	ASTM D 2471	160 °C	135.8 °C
Peak Time/Gel Time	ASTM D 3056	2	1.8
Solid Content (@300cp)	ISO 3344	64.09%	77.04%

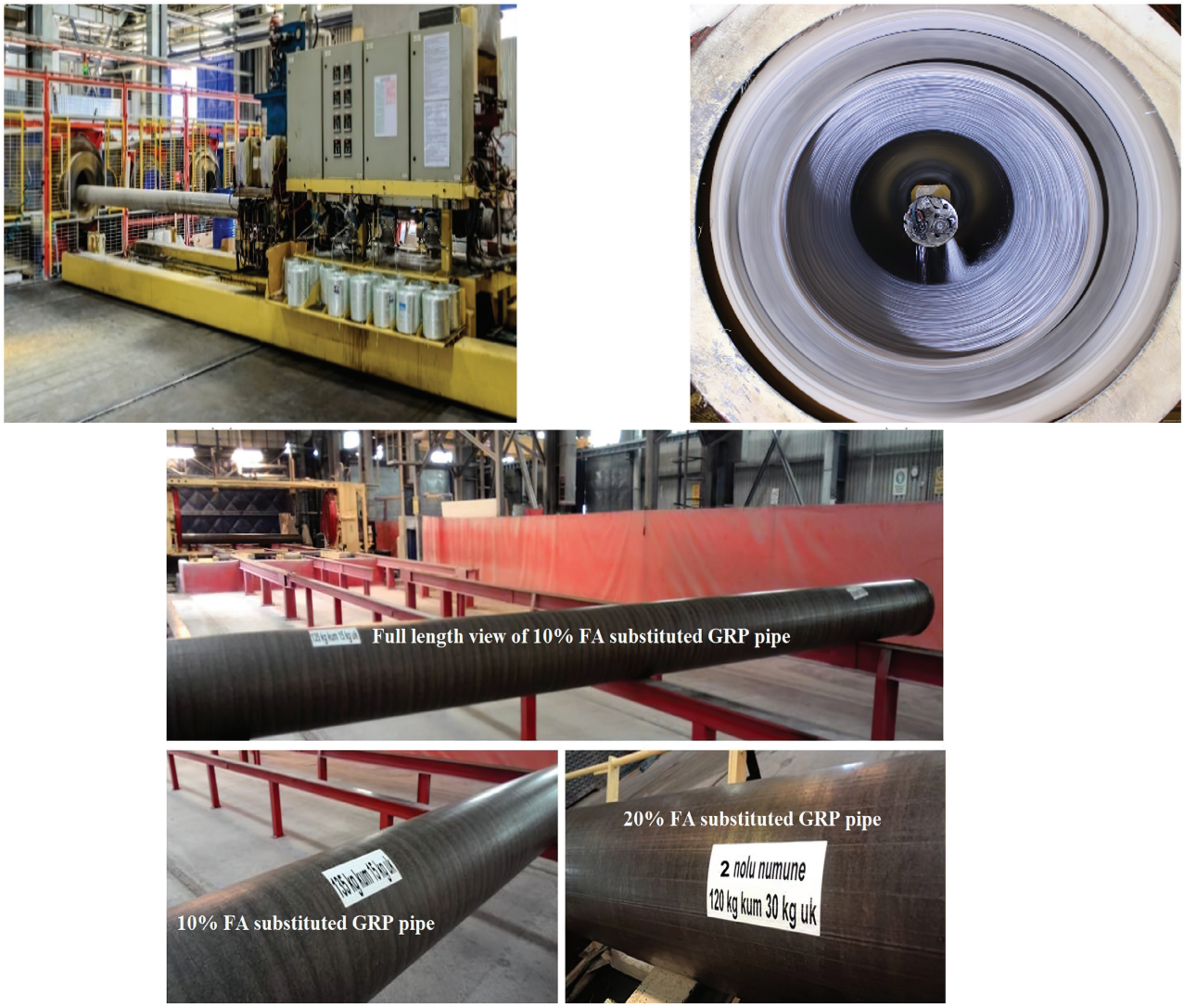

FIGURE 1. (a) - (b) General view of pipe production by CC method; (c) GRP pipe containing FA.

To calculate the stiffness modulus [S_m], Equation [3] was used. The parameter *f* in Equation [3] can be calculated using Equation [4].

$$S_m = \frac{f.F}{L.y} \quad [3]$$

$$f = \left\{1860 + \left(2500.\frac{y}{D_m}\right)\right\}.10^{-5} \quad [4]$$

f: Deflection coefficient
y: Deflection of the ring at maximum force (m)
F: Force (N) used to give the test specimen a deflection of 2.5 – 3.5%, based on mean diameter
L: Average ring length (m)

3. RESULTS AND DISCUSSION

3.1. Mechanical performance of GRP pipes

The SM test was performed to evaluate the rigidity of the GRP pipes and the results are given in Table 4. According to the table, the highest SM result was calculated as 6195 N/m^2 for the reference pipe, while the result was 7752 N/m^2 for the 10% FA pipe and 7701 N/m^2 for the 20% FA pipe. According to the mean values of all groups, the 10% FA substitution increased the SM results by 17.53%, whereas the 20% FA increased the SM results by 5.33% in comparison to the REF. In addition, the experimental results revealed that the 10% FA substitution was more effective on the SM results than the 20% FA substitution. Deflection ability without defects and cracks is also an

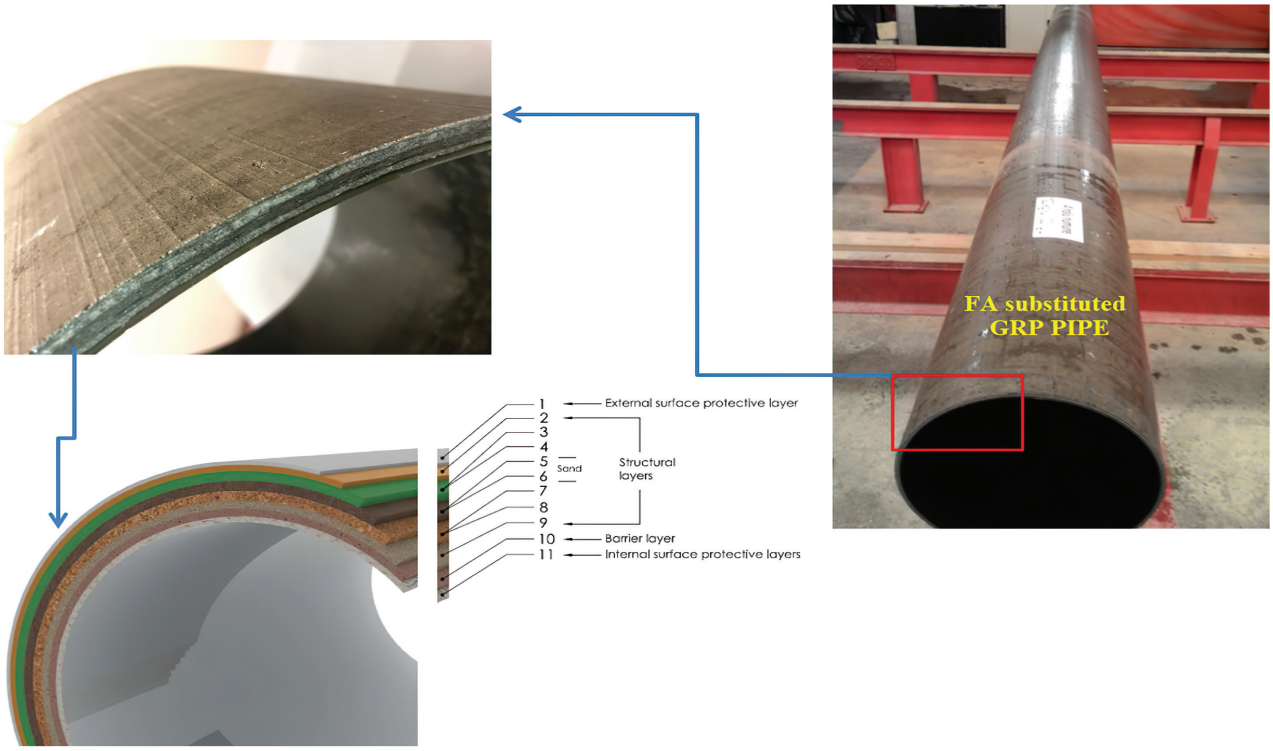

FIGURE 2. 10% FA-substituted GRP pipe with cross-sectional details.

TABLE 3. Description of tests and specifications.

Test /Specification	Sample Dimensions
SM ISO 7685	4 pieces: 30-cm wide (2 pieces at one end, 2 pieces at the other end)
HTS ISO 8521	20 pieces: 2.5-cm wide, as circle-shaped strips (10 pieces at one end, 10 at the other end of the pipe after cutting the stiffness samples)
ATS ISO 8513	20 pieces: 2 × 30 cm strips taken along the axis of the pipe (through the circumference of the remaining part of the pipe after cutting the samples, 10 from each end)

important property expected from pipes under the effects of strain. During the SM testing, no visual defects were observed on the pipes at 11.3% deflection and no structural cracks were observed on the pipes at 18.9% deflection.

When the SM test results were evaluated in terms of compatibility with the EN 1796 standard, it was seen that the GRP pipes produced with FA substitution met the 5000 N/m^2 requirement given in the EN 1796 standard. The SM results indicated that the use of FA in the production of GRP pipe is possible. Table 5 presents the results of the HTS and ATS tests. As seen in the table, the HTS results for the pipes ranged from 933.3 to 1326.9 N/mm for the REF, from 763.1 to 1400 N/mm for the 10% FA substitution, and from 632.9 to 1168.1 N/mm for the 20% FA substitution. The ATS results of the pipes varied from 132.1 to 186.9 N/mm for the REF, from 136 to 195.2 N/mm for the 10% FA substitution, and from 126.2 to 178.2 N/mm for 20% FA substitution. When the averages of all groups were evaluated, the 10% FA substitution led to a 3% decrease in the HTS, while the 20% FA substitution resulted in an 8% decrease, compared to the REF. Contrary to the HTS results, the 10% FA substitution caused a 6.8% increase in the ATS, while the 20% FA substitution led to a 1.47% increase.

3.2. Effect of the pipe layer thickness on mechanical performance

It was expected that the test results of samples taken from the same GRP pipe would be close to each other. When the HTS, ATS, SM, and EM results presented above were evaluated, it was observed that the results for samples taken from the same pipe exhibited a wide range of values. For example, in the

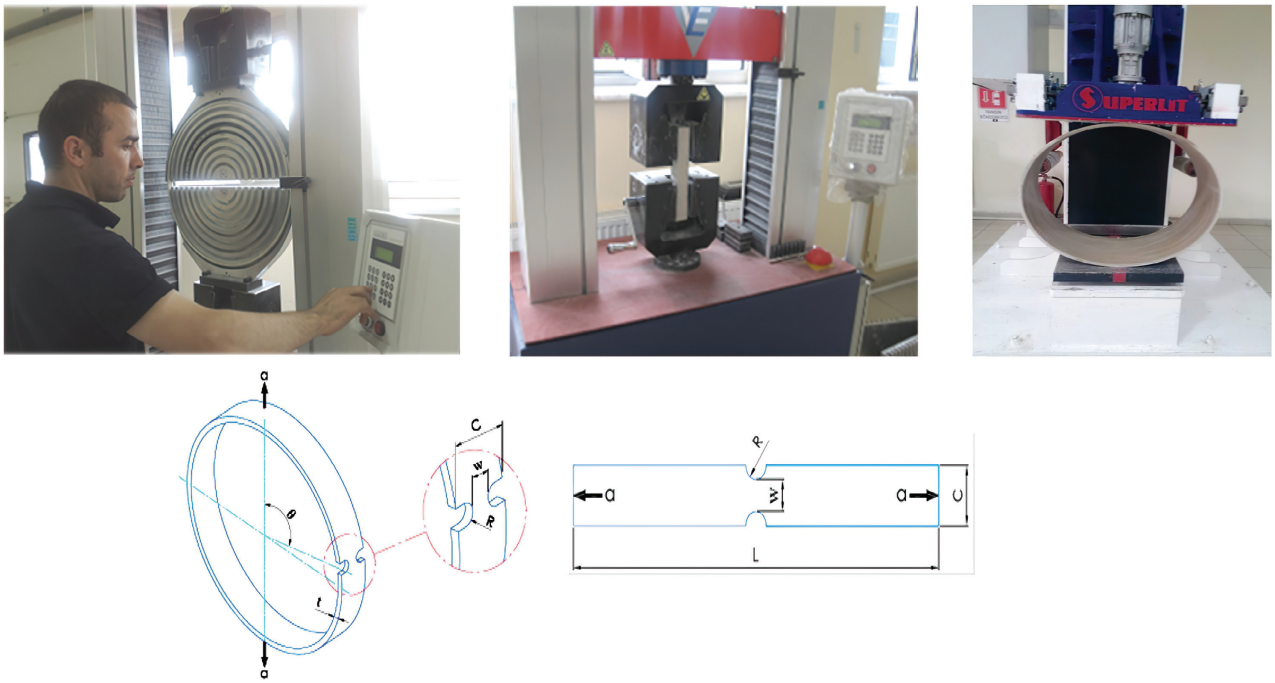

FIGURE 3. (a) HTS test; (b) ATS test; (c) SM test; (d) details of HTS test samples; (e) details of ATS test samples.

TABLE 4. SM results of GRP pipes.

	Width	Thickness	Force (F)	SM		
NO	**mm**	**mm**	**N**	**N/m^2**	**Level A***	**Level B****
REF	298	8.74	926	5465	No	No
	292	8.58	889	5352	No	No
	305	8.86	1074	6195	No	No
	296	8.78	1010	6001	No	No
10% FA	295	9.11	1299	7752	No	No
	298	9.17	1054	6227	No	No
	300	9.29	1105	6487	No	No
	294	9.19	1099	6582	No	No
20% FA	297	8.76	781	4625	No	No
	297	8.67	876	5186	No	No
	300	9.22	1312	7701	No	No
	295	9.2	1127	6727	No	No

* Level A: Visual defects at 11.3% deflection
** Level B: Structural cracks at 18.9% deflection

HTS tests performed on samples containing 10% FA, the results varied between 763.1 N/mm and 1198.1 N/mm. To analyze the reason for the standard deviation of the test results, a section was taken from each type of pipe, as shown in Figure 4, and these sections were examined via microscopic images.

The microscope images in Figure 4 clearly show the variations in layer thickness, which for the thinnest points of the layer were measured as 1.75 mm for REF, 1.98 mm for 10% FA, and 1.67 mm for 20% FA, while the thickest points were found as 2.03 mm, 2.36 mm, and 2.53 mm. The average layer thickness was calculated as 1.89 mm, 2.17 mm, and 2.10 mm for REF, 10% FA, and 20% FA, respectively. This variation resulted from the composite nature of the pipes. Layer thickness, especially in layers containing fibers, had an important effect on the mechanical properties of the GRP pipe. Since these differences in the thickness of the layers yielded a wide range of test results, it was difficult to interpret how FA use affected the mechanical

TABLE 5. HTS and ATS test results for GRP pipes.

	HTS Results (N/mm)					ATS Results (N/mm)				
	1	2	3	4	5	1	2	3	4	5
REF	1226.9	1145.6	1067.3	1070.2	1145.1	146.67	135.02	150.5	159.18	138.86
	1076.7	1201	1150.5	1009.6	1106.1	149.15	154.06	136.86	145.93	142.7
	933.3	943.4	1326.9	1183.7	1006.2	165.81	158.89	132.64	134.58	164.63
	1037.4	1260.6	1235.5	966.9	974.6	132.07	153.51	137.92	162.97	144.53
10% FA	1024.4	1205.4	1094.6	1062.3	1198.1	151.75	175	159.42	172.96	172.83
	1043.2	1098.8	1400	1131.7	763.1	146.6	151.14	164.11	140.64	136.27
	1137.46	1011.61	1083.31	774.5	828.13	177.03	186.89	164.46	165.01	138.88
	1142.92	940.34	972.89	931.8	1164.26	195.18	162.46	152.45	163.52	171.38
20% FA	947.08	1080.89	1075.64	1066.74	1162.24	158.36	149.78	157.84	126.21	170.08
	1160.92	1168.09	1042.04	1014	1040.65	154.85	139.65	137.5	145.77	154.31
	632.91	961.57	1039.56	836.53	1149.43	152.2	186.36	157.98	158.36	170.57
	1029.38	1040.02	815.43	977.93	1038.34	156.92	178.18	173.93	149.67	156.9

When the HTS and ATS results were compared with the lower limits of the standards (443 N/mm for HTS in AWWA C950 and 102 N/mm for ATS in EN 1796), it was observed that the results for all pipes were higher than the corresponding lower limits of the standards.

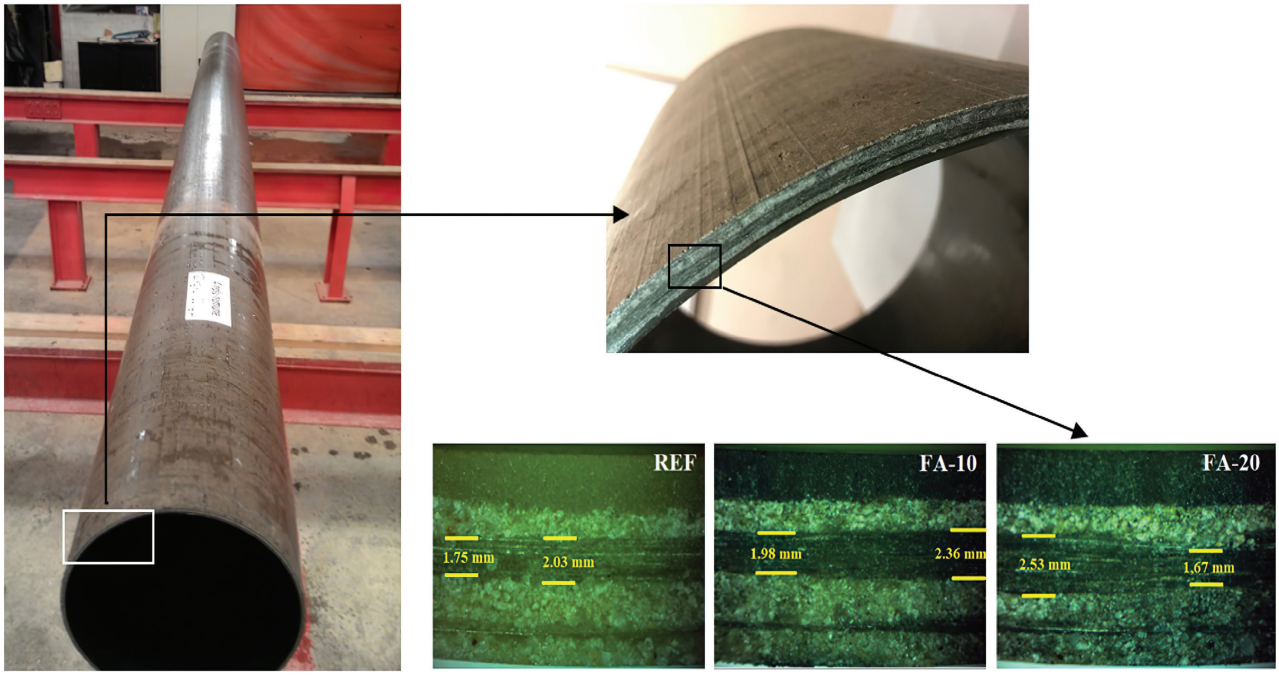

FIGURE 4. Cross-section and microscopic images showing cross-section details.

properties of the GRP pipe. In this respect, it was regarded as more meaningful to evaluate the adequacy of the mechanical performance of the FA-filled GRP pipe according to the related standards instead of merely comparing it to a reference pipe.

3.3. Microstructural and ITZ analyses

Within the scope of the microstructural analysis, scanning electron microscopic (SEM) images of the FA-filled GRP pipes are given in Figure 5. Figure 5 a shows the general view of the structural layer of the 20% FA-filled GRP pipe, and 5 b shows the bond between the FA and the resin. Figure 5 c-d shows the distribution of FA particles inside the resin matrix. As a cementitious material, FA is pozzolanic and reacts with water and CaOH. The figure shows that, as the microstructure of the composite does not contain water to react with the FA, the FA particles do not react with any other particles, and thus they can be easily seen in their spherical forms, homogeneously distributed in the resin matrix without any

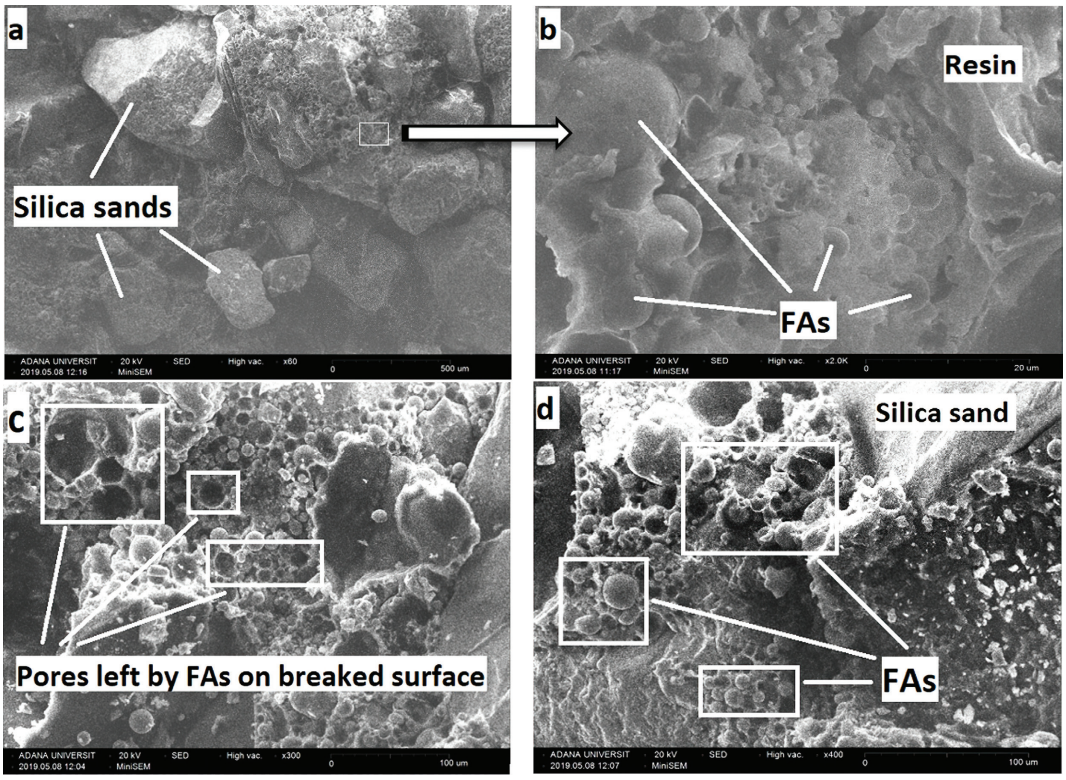

FIGURE 5. SEM images of the microstructure of the FA-filled GRP pipe.

agglomeration (Figure 5 c-d). Moreover, sufficient bondings are seen between the FA particles and the resin matrix (Figure 5 b). Several micro pores were observed on the broken surface (Figure 5 c-d) as the marks of FA particles.

The microstructures of all interfacial transition zones (ITZs) in a GRP pipe cross-section are given in Figure 6. In Figure 6 a, all layers of the GRP pipe were numbered to describe the ITZs. The first layer ("1") on the GRP thin section consists of pure resin and is the internal surface protective layer. Layers "2" – "5" are structural layers. Layers "2" and "4" are FA-filled layers containing silica sand + FA + resin, while layers "3" and "5" consist only of resin and glass fibers. These figures were prepared to evaluate the bond between the layers of the GRP pipes containing FA.

As seen in Figure 6 b-f showing the FA-filled GRP pipe, the resin covered the surface by penetrating into the rough areas. Hence, a good interfacial bond was formed. The sections with rough surface forms, as shown in the figures, are the sections containing silica sand. These rough surfaces are mainly related to the surface structure of the sand. In order to compare the ITZs of the FA-filled GRP pipe with the reference GRP pipe, the ITZ images of reference samples are given in Figure 6 g-i. Similar to the REF GRP pipe, no detachment, weak bonding, or visible defects were observed on the ITZs of the FA-filled GRP pipe. Moreover, the strong, dense structure of the ITZs of both the 20% FA and the REF pipes seem to be similar. It can be concluded that the use of FA does not adversely affect the bond between the layers.

3.4. Durability of FA-filled samples subjected to strain-corrosion testing

The samples of reference GRP pipe and 20% FA GRP pipe were tested according to ASTM D3681. A schematic illustration of the test is given in Figure 7. This test method evaluates the effect of a chemical environment on a pipe in a deflected condition. Generally, this experiment can last up to 10,000 h, but in this study, the experiment was modified at the initial level in order to make relative comparisons of the 20% FA GRP pipe and the reference GRP pipe. This practice was carried out in order to present the findings of this study, with its comprehensive experimental content, to the literature without delay.

In the experiments, the samples were placed in the test apparatus with the measured wall thicknesses at the bottom and the force was applied to the apparatus to deflect the samples while keeping the top and bottom plates of the apparatus as nearly parallel as possible. When the desired deflection was obtained, the apparatus was locked to maintain the sample in the deflected condition. An addition of 1N sulfuric

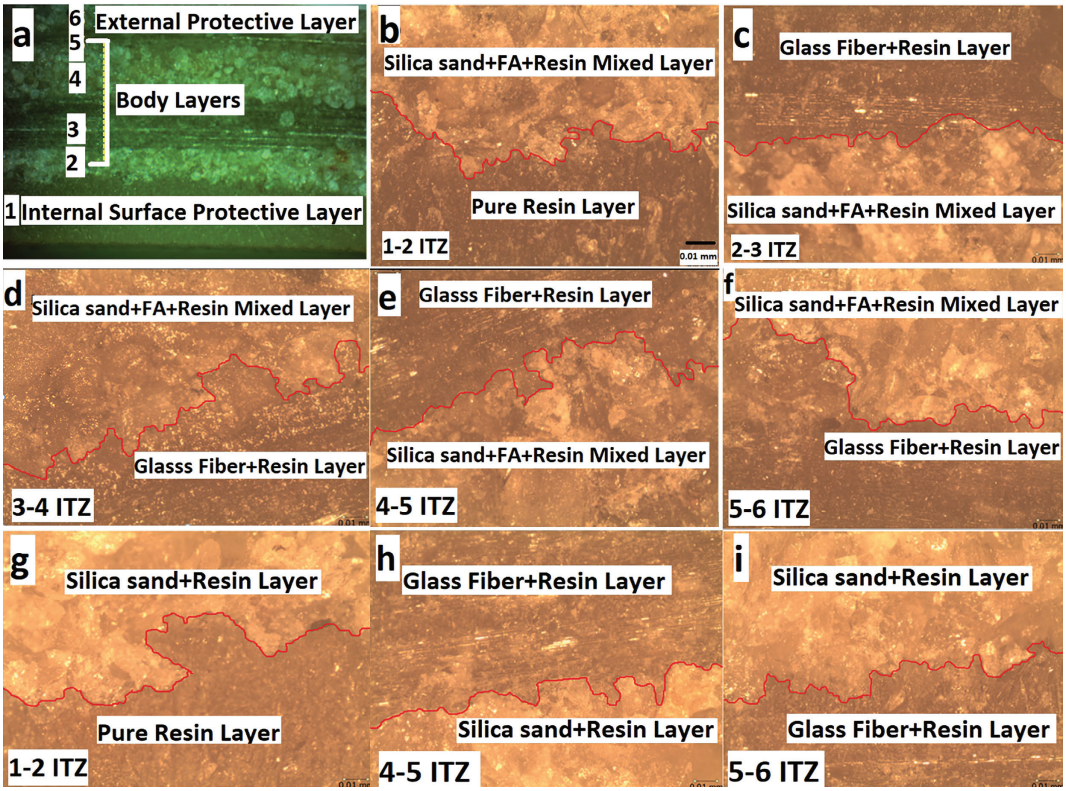

FIGURE 6. Optical microscopic images of ITZs in GRP pipe layers.

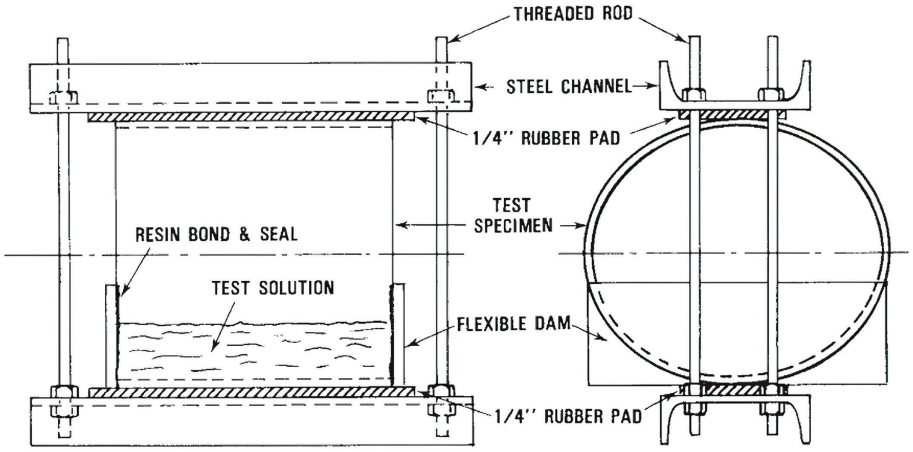

FIGURE 7. Schematic illustration of strain-corrosion test.

acid (H_2SO_4) was introduced into the test frame. The vertical deflection degree applied to the samples in order to achieve a failure at between 100 h and 600 h was calculated as 21.5%, which, through experience, was seen as an expected value. Figure 8 a-b shows the application of the test on the reference GRP pipe and the 20% FA GRP pipe, respectively.

The pipe samples were checked and controlled at every 6 h. After exceeding the expected time to failure (100–600 h), the strain-corrosion test was terminated after 1029 h. Initial observations showed that the FA content did not have a negative effect on the durability of the GRP pipe.

In addition to the above-mentioned application, after terminating the strain-corrosion test at 1029 h, the vertical deflection was applied to the samples until visual cracks and structural failure occurred in order to make a relative comparison between the

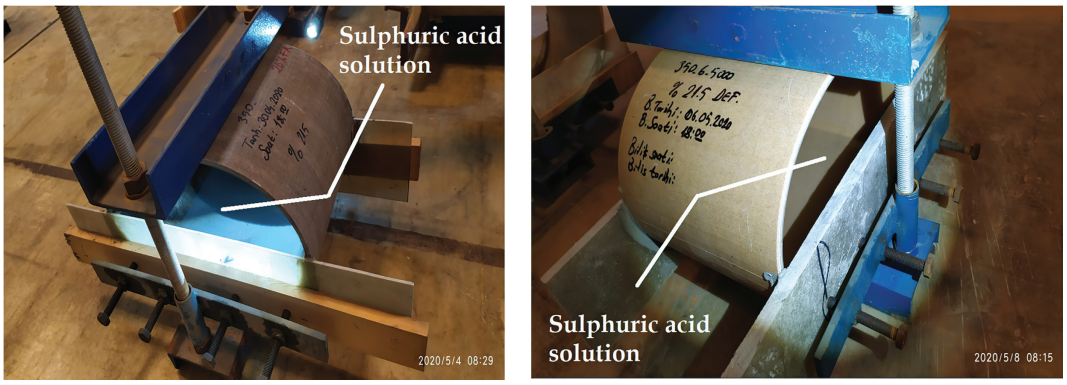

FIGURE 8. Application of the strain-corrosion test on the GRP samples.

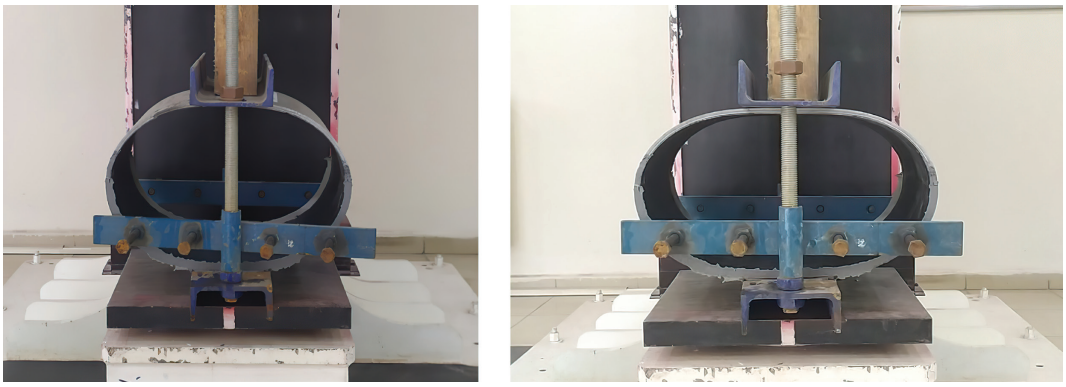

FIGURE 9. Sample images of the deflection application.

mechanical performances of the pipes following the effect of an acidic environment.

In order to determine the visual crack deflection level (%) and structural failure deflection level (%), additional deflections were applied with a 1% increase in addition to the 21.5% initial deflection on the samples. Sample images of the deflection application with specific increases are seen in Figure 9.

The visual crack deflection level of the 20% GRP pipe sample was found to be 41.5%. Later, the number of cracks increased rapidly and the deflection level of the failure was observed as 46.5%. Figure 10 a-b shows the surface cracks and failure of the sample, respectively. The visual crack deflection level and structural failure deflection level were found as 38.5% and 41.5% for the reference GRP pipe, respectively. The surface cracks and failure of the reference GRP pipe are seen in Figure 10 c-d.

The results obtained seemed to indicate that the performance of the GRP pipes containing FA after the effect of the acidic environment was acceptable, and similar to that of the reference GRP pipe. The slightly higher deflection values found in the GRP pipe containing FA compared to the reference GRP pipe were not sufficient enough to conclude that the performance of the FA-filled GRP pipe was better than the reference GRP pipe. This difference may have been related to the effect of the pipe layer thickness, as explained in section 3.2.

4. CONCLUSIONS

Since natural raw material resources are limited, the use of recycled materials in industrial production is very important for sustainability. Various types of recycled materials are currently being used in many branches of engineering. Civil engineering is one of the leading engineering fields in the utilization of large amounts of solid wastes. According to this experimental investigation carried out to evaluate the potential reusability of FA in the production of GRP pipes, the following conclusions can be drawn:

- For all GRP pipes (including FA-filled GRP pipes), no visible damage was observed at a deflection level of 11.3% and no structural cracks at a deflection level of 18.9%.
- The 10% FA substitution increased the SM results by 17.53%, while the 20% FA substitution increased them by 5.33%.
- The 10% FA substitution decreased the HTS results by 3%, while the 20% FA substitution decreased them by 8%.

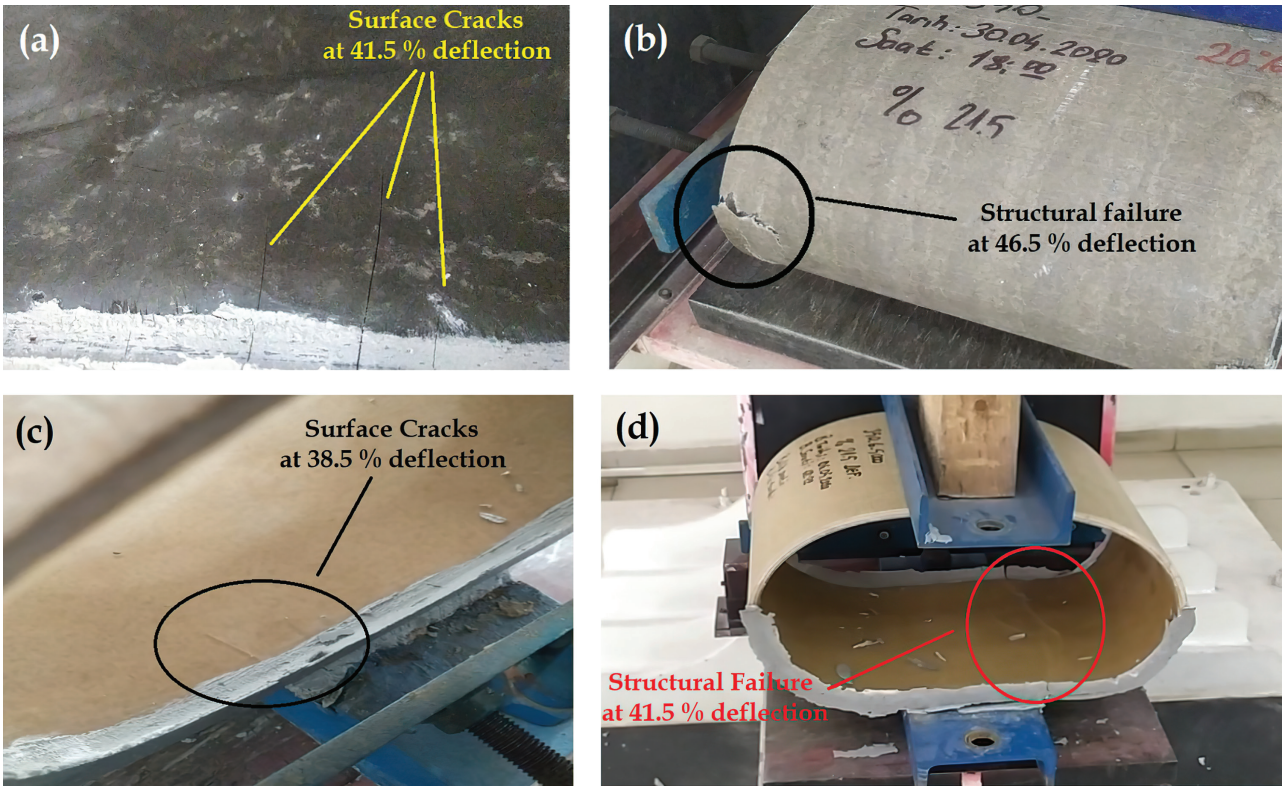

FIGURE 10. Crack propagation and failure in the samples after acid effect.

- The 10% FA substitution increased the ATS results by 6.8% while the 20% FA substitution increased them by 1.47%.
- When the results of SM, HTS, and ATS were evaluated together, it was difficult to conclude whether or not the FA substitution had increased the mechanical properties. However, all results showed that both 10% and 20% substitution ratios of FA were suitable for the production of GRP pipes that meet the related standards. Determining the adequacy of mechanical performance of FA-filled GRP pipes within the scope of related standards is more meaningful than comparing their performance with a reference pipe.
- The SEM images showed that it was possible to achieve the homogeneous distribution of FA particles within the resin matrix without any agglomeration.
- According to the microstructural analysis, sufficient interfacial bonding was observed between the resin matrix and the FA.
- According to the ITZ analysis, in both in the REF and the FA-filled GRP pipes, the resin had penetrated into the rough surfaces and formed a good interfacial bond. It can be concluded that the use of FA does not adversely affect the bond between the layers.
- The results of the strain-corrosion test indicated that the performance of the FA-filled GRP pipes after the effect of the acidic environment was acceptable, and similar to that of the reference GRP pipe.
- The use of FA in GRP pipes reduces the demand on raw materials such as silica sand.
- In addition to well-known conventional studies related to the use of FA in cement and concrete, the use of FA in GRP production presented in this study can open a new path for the consumption of FA in a useful way.

All findings of this experimental study indicate that the use of FA in GRP pipe production is possible. Low-lime FA (Class F, having CaO<10% according to ASTM C618) was used in this study. Because of its high pozzolanic activity, low-lime FA is commonly used rather than high-lime FA (Class C, having CaO>10% according to ASTM C618). It is recommended that future research should focus on the potential use of high-lime FA, which has a relatively low pozzolanic activity, in GRP pipe production.

ACKNOWLEDGEMENTS

The authors would like to thank the management of Superlit Pipe Industry Inc. for their support in producing and testing all GRP pipes.

REFERENCES

1. Ahmaruzzaman, M. (2010) A review on the utilization of fly ash. *Prog. Energy Combust. Sci*. 36 [3], 327–363. https://doi.org/10.1016/j.pecs.2009.11.003.
2. Dindi, A.; Quang, D.V.; Vega, L.F.; Nashef, E.; Abu-Zahra, M.R.M. (2019) Applications of fly ash for CO_2 capture, utilization, and storage. *J. CO_2 Util.* 29, 82–102. https://doi.org/10.1016/j.jcou.2018.11.011.
3. Basu, M.; Pande, M.; Bhadoria, P.B.S.; Mahapatra, S.C. (2009) Potential fly-ash utilization in agriculture: A global review. *Prog. Nat. Sci.* 19 [10], 1173–1186. https://doi.org/10.1016/j.pnsc.2008.12.006.
4. Xie, J.; Wang, J.; Rao, R.; Wang, C.; Fang, C. (2019) Effects of combined usage of GGBS and fly ash on workability and mechanical properties of alkali activated geopolymer concrete with recycled aggregate. *Compos. Part B. Engineer*. 164, 179–190. https://doi.org/10.1016/j.compositesb.2018.11.067.
5. Bicer, A. (2018) Effect of fly ash particle size on thermal and mechanical properties of fly ash-cement composites. *Therm. Sci. Eng. Prog.* 8, 78–82. https://doi.org/10.1016/j.tsep.2018.07.014.
6. Cheng, Q.; Yao, K.; Liu, Y. (2018) Stress-dependent behavior of marine clay admixed with fly-ash-blended cement. *Int. J. Pavement Res. Technol.* 11 [6], 611–616. https://doi.org/10.1016/j.ijprt.2018.01.004.
7. Martin, L.H.J.; Winnefeld, F.; Tschopp, E.; Müller, C.J.; Lothenbach, B. (2017) Influence of fly ash on the hydration of calcium sulfoaluminate cement. *Cem. Concr. Res.* 95, 152–163. https://doi.org/10.1016/j.cemconres.2017.02.030.
8. Güllü, H.; Cevik, A.; Al-Ezzi, K.M.A.; Gülsan, M.E. (2019) On the rheology of using geopolymer for grouting: A comparative study with cement-based grout included fly ash and cold bonded fly ash. *Constr. Build. Mater.* 196, 594–610. https://doi.org/10.1016/j.conbuildmat.2018.11.140.
9. Duan, S.; Liao, H.; Ma, Z.; Cheng, F.; Fang, L.; Gao, H.; Yang, H. (2018) The relevance of ultrafine fly ash properties and mechanical properties in its fly ash-cement gelation blocks via static pressure forming. *Constr. Build. Mater.* 186, 1064–1071. https://doi.org/10.1016/j.conbuildmat.2018.08.035.
10. Ren, X.; Sancaktar, E. (2019) Use of fly ash as eco-friendly filler in synthetic rubber for tire applications. *J. Clean. Prod.* 206, 374–382. https://doi.org/10.1016/j.jclepro.2018.09.202.
11. Zhang, H.; Shen, C.; Xi, P.; Chen, K.; Zhang, F.; Wang, S. (2018) Study on flexural properties of active magnesia carbonation concrete with fly ash content. *Constr. Build. Mater.* 187, 884–891. https://doi.org/10.1016/j.conbuildmat.2018.08.017.
12. Sun, Z.; Vollpracht, A. (2019) One year geopolymerisation of sodium silicate activated fly ash and metakaolin geopolymers. *Cem. Concr. Compos.* 95, 98–110. https://doi.org/10.1016/j.cemconcomp.2018.10.014.
13. Wang, W.; Lu, C. (2018) Time-varying law of rebar corrosion rate in fly ash concrete. *J. Hazard. Mater.* 360, 520–528. https://doi.org/10.1016/j.jhazmat.2018.08.007.
14. Hadi, M.N.S.; Al-Azzawi, M.; Yu, T. (2018) Effects of fly ash characteristics and alkaline activator components on compressive strength of fly ash-based geopolymer mortar. *Constr. Build. Mater.* 175, 41–54. https://doi.org/10.1016/j.conbuildmat.2018.04.092.
15. Hefni, Y.; El Zaher, Y.A.; Wahab, M.A. (2018) Influence of activation of fly ash on the mechanical properties of concrete. *Constr. Build. Mater.* 172, 728–734. https://doi.org/10.1016/j.conbuildmat.2018.04.021.
16. Bahedh, M.A.; Jaafar, M.S. (2018) Ultra high-performance concrete utilizing fly ash as cement replacement under autoclaving technique. *Case Stud. Constr. Mater.* 9, e00202. https://doi.org/10.1016/j.cscm.2018.e00202.
17. Gökçe, H.S.; Hatungimana, D.; Ramyar, K. (2019) Effect of fly ash and silica fume on hardened properties of foam concrete. *Constr. Build. Mater.* 194, 1–11. https://doi.org/10.1016/j.conbuildmat.2018.11.036.
18. Uysal, M.; Akyuncu, V.; Tanyildizi, H.; Sumer, M.; Yildirim, H. (2018) Optimization of durability properties of concrete containing fly ash using Taguchi's approach and Anova analysis. *Rev. Construcc.* 17 [3], 364–382. http://doi.org/10.7764/rdlc.17.3.364.
19. Atis, C.D.; Bilim, C.; Ozcan, F.; Akcaozoglu, K.; Sevim, U.K. (2002) The use of a non-standard high calcium fly ash in concrete and its response to accelerated curing. *Mater. Construcc.* 52 [267], 5–17. https://doi.org/10.3989/mc.2002.v52.i267.322.
20. Irassar, E.F.; Batic, O.R. (1989) Sulfate resistance of ordinary Portland cement with fly ash. *Mater. Construcc.* 39 [213], 11–20. https://doi.org/10.3989/mc.1989.v39.i213.813.
21. Fernández-Jiménez, A.; Palomo, A.; Criado, M. (2006) Alkali activated fly ash binders. A comparative study between sodium and potassium activators. *Mater. Construcc.* 56 [281], 51–65. http://doi.org/10.3989/mc.2006.v56.i281.92.
22. Woszuk, A.; Bandura, L.; Franus, W. (2019) Fly ash as low cost and environmentally friendly filler and its effect on the properties of mix asphalt. *J. Clean. Prod.* 235, 493–502. https://doi.org/10.1016/j.jclepro.2019.06.353.
23. Yan, K.; Li, L.; Zheng, K.; Ge, D. (2019) Research on properties of bitumen mortar containing municipal solid waste incineration fly ash. *Constr. Build. Mater.* 218, 657–666. https://doi.org/10.1016/j.conbuildmat.2019.05.151.
24. Zacco, A.; Borgese, L.; Gianoncelli, A.; Struis, R.P.W.J.; Depero, L.E.; Bontempi, E. (2014) Review of fly ash inertisation treatments and recycling. *Environ. Chem. Lett.* 12, 153–175. https://doi.org/10.1007/s10311-014-0454-6.
25. Mazzoli, A.; Moriconi, G. (2014) Particle size, size distribution and morphological evaluation of glass fiber reinforced plastic (GRP) industrial by-product. *Micron.* 67, 169–178. https://doi.org/10.1016/j.micron.2014.07.007.
26. Colombo, C.; Vergani, L. (2018) Optimization of filament winding parameters for the design of a composite pipe. *Compos. Part B. Engineer.* 148, 207–216. https://doi.org/10.1016/j.compositesb.2018.04.056.
27. Tittarelli, F.; Moriconi, G. (2010) Use of GRP industrial by-products in cement based composites. *Cem. Concr. Compos.* 32 [3], 219-225. https://doi.org/10.1016/j.cemconcomp.2009.11.005.